THE AMERICAN SOCIETY OF MECHANICAL ENGINEERS
345 E. 47th St., New York, N.Y. 10017

98-GT-409

TESTING, ANALYSIS, AND CFD MODELING OF A PROFILED LEADING EDGE GROOVE TILTING PAD JOURNAL BEARING

Stephen L. Edney
Dresser-Rand Company
37 Coats St., Wellsville, N.Y.
email: stephen_l_edney@dresser-rand.com

Gregory B. Heitland
Dresser-Rand Company
37 Coats St., Wellsville, N.Y.
email: greg_b_heitland@dresser-rand.com

Scan M. DeCamillo
Kingsbury, Inc.
10385 Drummond Road
Philadelphia, PA 19154

ABSTRACT

Testing and analysis of a profiled leading edge groove tilting pad journal bearing developed for light load operation is described. This bearing was designed for a generic, small, high speed steam turbine operating at projected loads of less than 25 psi (172.4 kPa) and journal surface speeds to 400 ft/s (122 m/s). On the second turbine application, a rotor instability was experienced with the oil flowrate reduced to optimize bearing steady state performance. This instability was eliminated by machining a taper on the exit side of the feed groove on each pad. At the reduced flowrate, the profiled groove bearing greatly improved the operating characteristics of the rotor system by reducing vibration amplitudes and stabilizing operation at speed.

This paper is divided into two sections. The first section compares the rotordynamics analysis with test data that shows improved unbalance response and operating stability with the profiled groove bearing. The second section provides original insight of the effect of the profiled geometry on the bearing flow field using computational fluid dynamics models.

INTRODUCTION

As machine speeds have increased to pursue improved performance in turbomachinery, so have the challenges in rotor and bearing design. Higher operating speeds direct the development of smaller machines that introduce constraints to the rotor design. Accordingly, the applicable limits of conventional flooded bearings can be stretched, especially when operation extends into the turbulent flow regime. Bearing losses increase exponentially with turbulent flow which can negatively impact a machine's overall efficiency. Likewise, high bearing temperatures can approach the limits of the babbitt. This is a particular concern to OEMs and users of turbomachinery since the safety margin against failure may be reduced.

Presented herein is a case history of a leading edge groove tilting pad journal bearing used in a generic, small, high speed steam turbine. Directed lubrication leading edge groove bearings were used to address temperature concerns at the high journal surface speeds (approaching 400 ft/s (122 m/s)). Specifically discussed is a pad modification to eliminate a bearing induced instability in an application with significantly reduced oil flowrate.

Trend in Bearing Design

The requirements for new bearing designs are clear: increased load carrying capacity and lower frictional losses at reduced oil flowrate. These requirements are to be met without increasing operating pad temperature. Bearing manufacturers initially focused their efforts on improving the thrust bearing design, Mikula (1981). Thrust bearings were the logical starting point since they account for the majority of the losses in the total bearing system. These new designs first utilized the concept of directed lubrication technology, and have been widely used on OEM machinery over the last decade.

It has only been in the last few years that this new technology has been applied to tilting pad journal bearings as described by Tanaka (1991), Harangozo (1991), and Dmochowski (1993). Machine speeds are now approaching the limits of acceptable performance of conventional flooded designs, Edney (1995), particularly when operation extends into the turbulent flow regime. Under these conditions, bearing losses increase

Presented at the International Gas Turbine & Aeroengine Congress & Exhibition
Stockholm, Sweden — June 2–June 5, 1998

exponentially which can have a noticeable effect on a machine's overall efficiency. Increasing the oil flowrate to reduce high bearing temperatures increases the losses further, and the size and cost of the lubrication system with minimal benefit.

GENERIC HIGH SPEED STEAM TURBINE

The product specification for the turbine utilizing the leading edge groove bearings was for a design capable of producing up to 7000 hp (5.2 MW) and operating up to a maximum speed of 18000 rpm. A primary objective of this project was to develop, with minimal hardware change, a generic steam turbine design. This allows several combinations of steam and exhaust end assembly, single or multi valve inlet, and backpressure to condensing steam paths. A modular approach was used by fixing the bearing span and standardizing the steam and exhaust end bearing cases. A typical configuration is illustrated in Figure 1 of a single valve, five stage condensing design.

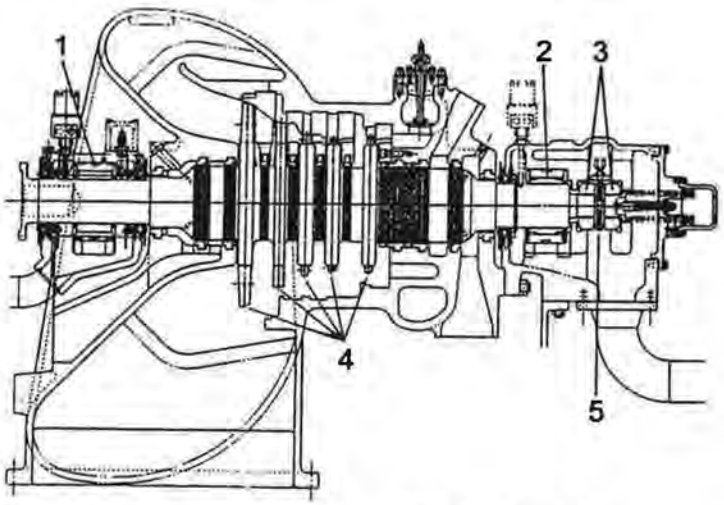

1 – Journal Bearing
2 – Journal Bearing
3 – Thrust Bearing
4 – Bladed Disks
5 – Thrust Collar

Fig. 1 Typical High Speed, Multistage, Steam Turbine

Rotor Design

To attain a maximum operating speed of 18000 rpm in compliance with current rotordynamics specifications (API, 1995), the bearing span and overhangs were kept to a minimum and the shaft diameter through the journal bearings increased. A base design was developed with a 51.0 inch (1.3 m) bearing span and 5.0 inch (12.7 cm) diameter journals. The midshaft diameter was left variable to allow tuning of the rotordynamic characteristics in relation to the operating speed range.

To minimize the steam end overhang and eliminate a toothed wheel, speed pickup teeth were machined onto the outside diameter of the thrust collar. The thrust bearing was kept as small as possible by stepping down the shaft diameter outboard of the journal. The shaft end was flanged to provide a face for axial displacement probes, with provision for grounding brushes near the axial centerline. The exhaust end overhang was minimized by tucking the bearing case under the diffuser portion of the exhaust. Two radial displacement probes were included just inboard of each journal bearing, 45° either side of top dead center. Two trim balance planes were provided as standard, one located at each end of the central shaft section.

Bearing Design

The journal bearings, illustrated in Figure 2, were leading edge groove five pad, 5.0 inch (12.7 cm) diameter by 3.75 inch (9.525 cm) long, load between pivot. The design diametral bearing clearance and pad preload were nominally 9.25 mil (0.235 mm) and 0.33, respectively. These parameters were originally determined from a sensitivity study of bearing geometry on rotor response. Oversize drain slots were machined into the bottom of the housing to allow spent hot oil to exit without partially flooding the bearing. Depending on rotor configuration, the projected load on each journal bearing could be in the range of 15 to 25 psi (103 to 172 kPa).

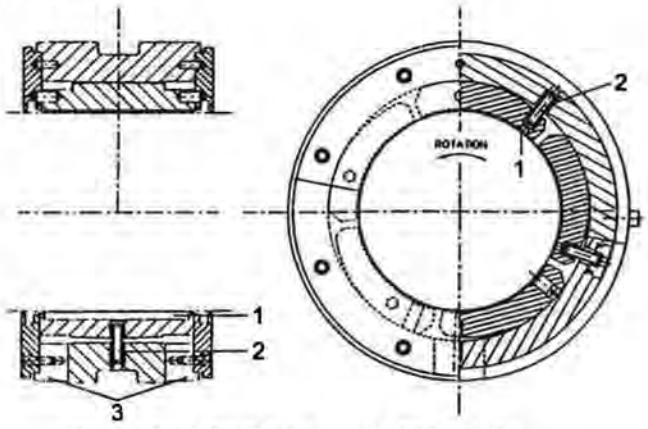

1 – Leading Edge Groove
2 – Feed Tube
3 – Drain Slot

Fig. 2 Leading Edge Groove Tilting Pad Journal Bearing

The thrust bearing, shown in Figure 3, was a leading edge groove self equalizing type with six pads with 12.5 inch^2 (80.6 cm^2) total area per side. Although the primary purpose for using these bearings was to reduce operating pad temperatures, reduced oil flowrates and bearing losses were also requirements. These latter two can contribute to a smaller lubrication system with associated cost savings.

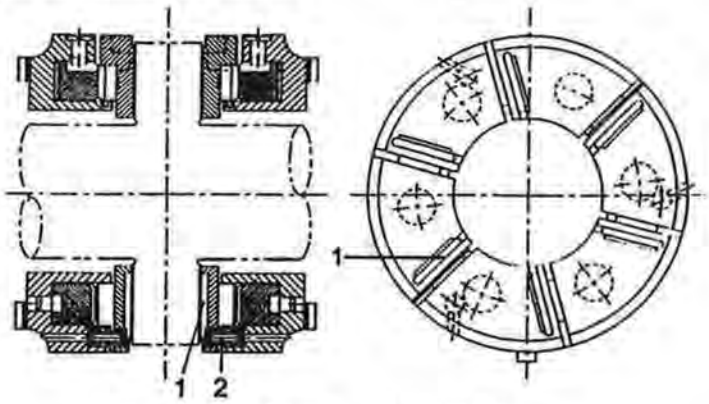

1 – Leading Edge Groove
2 – Feed Tube

Fig. 3 Leading Edge Groove Tilting Pad Thrust Bearing

First Production Application

The first production application using leading edge groove bearings was a three stage backpressure turbine with a rated power of 2568 hp (1.9 MW). The design operating range was from a minimum governor speed of 6826 up to a maximum continuous speed of 14335 rpm. The bearings were designed for a 15 psig (103 kPa) supply pressure and 120°F (49°C) inlet temperature; the lubricant was a light turbine oil. The oil flowrate to each journal bearing was approximately 7.5 gpm (28.4 liter/min), which is approximately 65 percent of that normally required by a flooded design. This unit ran successfully with trouble free operation up to the design trip speed of 15768 rpm.

A comparison of the analytical results and test measurements showed a reasonable response correlation. The location of the measured peak response speeds coincided within a few hundred rpm of the prediction. One apparent discrepancy, however, was the observed amplification factors. The four radial vibration probes indicated amplification factors three times higher than predicted, and did not indicate a critically damped response. A detailed discussion is given by Edney (1996), together with a review of the rotordynamics analysis.

Second Production Application

The second production application also was a three stage backpressure turbine but with a rated power of 5037 hp (3.7 MW). The design operating range was from a minimum governor speed of 9785 up to a maximum continuous speed of 12843 rpm. The steady state bearing performance was further optimized by reducing the oil flowrate through each journal bearing to 4.8 gpm (18.2 liter/min). This was achieved by reducing the oil supply pressure to 7.5 psig (51 kPa). The oil inlet temperature was 120°F (49°C), and the lubricant a light turbine oil.

The mass elastic model generated for the rotordynamics analysis is shown in Figure 4. The rotor was an integrally forged design with a 6.5 inch (16.5 cm) midshaft diameter. The model included the weight of all external components such as the blading and taper hydraulic fit coupling. The total rotor weight was 643 lb (292 kg), yielding specific pad loads of 18.0 psi (124 kPa) at the exhaust end and 16.3 psi (112.4 kPa) at the steam end. A support stiffness of 3.0×10^6 lb/in (5.25×10^6 N/cm) and mass of 150 lb (68 kg) were included at each bearing.

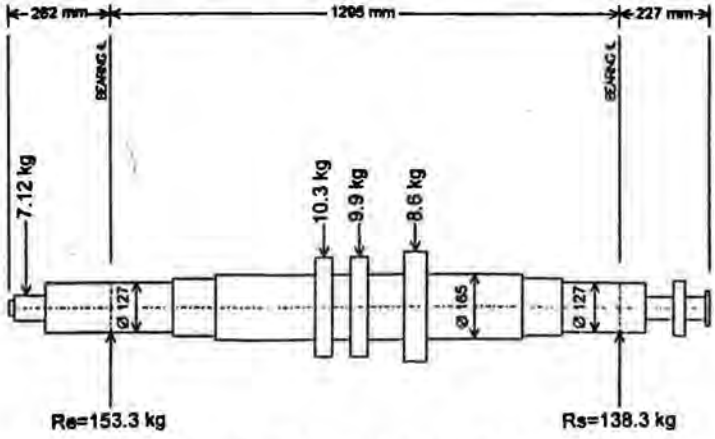

Fig. 4 Mass Elastic Model of Rotor

Stability

The results of an eigenvalue stability analysis at nominal bearing clearance are shown in Figure 5. The results are for the first forward whirl mode and associated logarithmic decrement. Intersection with the synchronous response line gives an approximate first forward damped lateral natural frequency of 6500 rpm. The logarithmic decrement indicates that the rotor-bearing system should be stable well beyond the maximum operating speed of 12843 rpm.

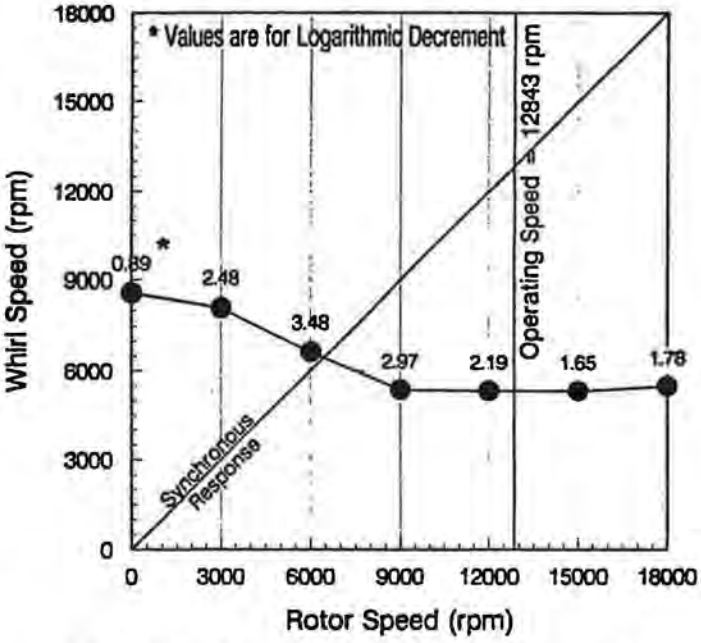

Fig. 5 Whirl Speed and Logarithmic Decrement Vs. Rotor Speed

During overspeed testing on this unit the rotor-bearing system went unstable at an operating speed of approximately 14000 rpm. With further attempts to run above the maximum operating speed, the speed at which the system went unstable decreased. The instability frequency coincided approximately with the rotor's first lateral natural frequency of 7500 rpm. Figure 6 illustrates a typical spectrum plot of observed frequency components at the maximum continuous operating speed of 12843 rpm.

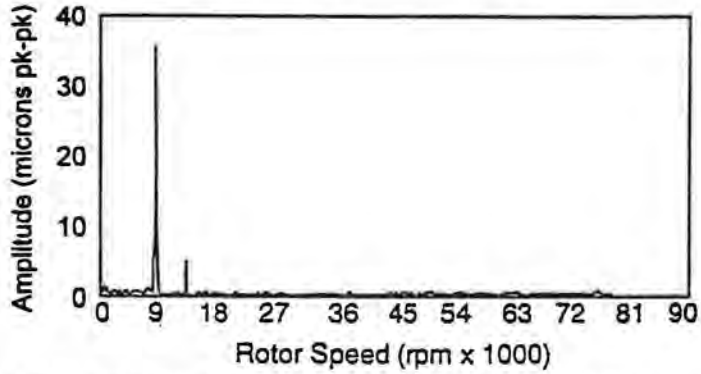

Fig. 6 Frequency Spectrum at 12843 rpm with Original Groove - Steam End Left Probe

This figure shows a synchronous amplitude of less than 0.2 mil (0.005 mm) pk-pk and a subsynchronous component reaching 1.4 mil (0.035 mm) pk-pk. At the time the machine went unstable, the subsynchronous component developed instantaneously and appeared as a pure spike. Higher subsynchronous amplitudes were reached with prolonged running.

Instability Phenomenon

The precise mechanism initiating the instability was not determined. A theory is that the combination of high journal surface speed (> 300 ft/s (91.4 m/s)) and extremely light pad load (< 25 psi (172 kPa)) contributed to this phenomenon. Under these conditions, the journal is highly centered in the bearing and the pad attitude angle very small. If this angle were small enough, a divergent region would exist near the trailing edge of the statically loaded pads. A film pressure would then be produced with a center that does not pass through the pivot. The resulting moment on the pad would cause it to pitch, producing a self excited unstable condition. Oil flowrate and/or supply pressure are the primary factors that contributed to this, since it was only the second application with reduced flowrate that exhibited the instability.

Since the pads were designed with a positive preload, pad flutter of the upper half (statically unloaded) pads was eliminated as a possible cause of the instability. Classical pad flutter occurs on upper pads when they become unloaded due to the loss of hydrodynamic load. This condition arises when a tilt angle cannot be reached for the pads to be in equilibrium. The pads were designed with a preload of 0.33, which would require a bearing eccentricity ratio of greater than 0.49 for the upper most pad to lose its capacity to generate a hydrodynamic load per Nicholas (1994). With the small pad loads involved, the bearing eccentricity ratio was predicted to be quite small (< 0.15 at 12843 rpm). This ensured some hydrodynamic load generation on the upper pads. The small operating eccentricity ratio was confirmed by measurement of journal position from change in DC gap voltage at the radial displacement probes. Pad flutter was first analytically addressed by Adams (1983) in a parametric study of statically unloaded pad vibration.

Bearing Pad Modification

The instability on the second application was eliminated by increasing the lubricant supply pressure and hence flowrate. The first application indicated this by running successfully at a higher supply pressure. At 15 psig (103 kPa) with a flowrate of 7.5 gpm (28.4 liter/min), the rotor ran smoothly at speeds well beyond 14000 rpm with no detectable sign of the subsynchronous vibration. The minimum supply pressure yielding stable operation appeared to be in the range of 11 to 12 psig (75.8 to 82.7 kPa). Unfortunately, increasing the oil supply pressure was not a viable option in the second application since additional flowrate was not available from the lubrication system. Consequently, a geometry modification to the leading edge groove was developed to stabilize performance. This modification, illustrated in Figure 7, consisted of machining a taper adjacent to the exit side of the groove of each pad. The objective of adding the taper was to improve flow entrance conditions and increase the operating pad attitude angle by creating an additional force at the pad leading edge. The additional force may be a result of a hydrodynamic oil film wedge or increased hydrostatic pressure in the tapered area. The modification proved successful with trouble free operation up to a maximum speed of 15500 rpm (journal surface speed of 338 ft/s (103 m/s)) at the design supply pressure of 7.5 psig (51.7 kPa). Design constraints of the blading prohibited operation at higher speeds on this unit. An equivalent spectrum plot at 12843 rpm is illustrated in Figure 8. There is no sign of the subsynchronous vibration with the synchronous amplitude again less than 0.2 mil (0.005 mm) pk-pk.

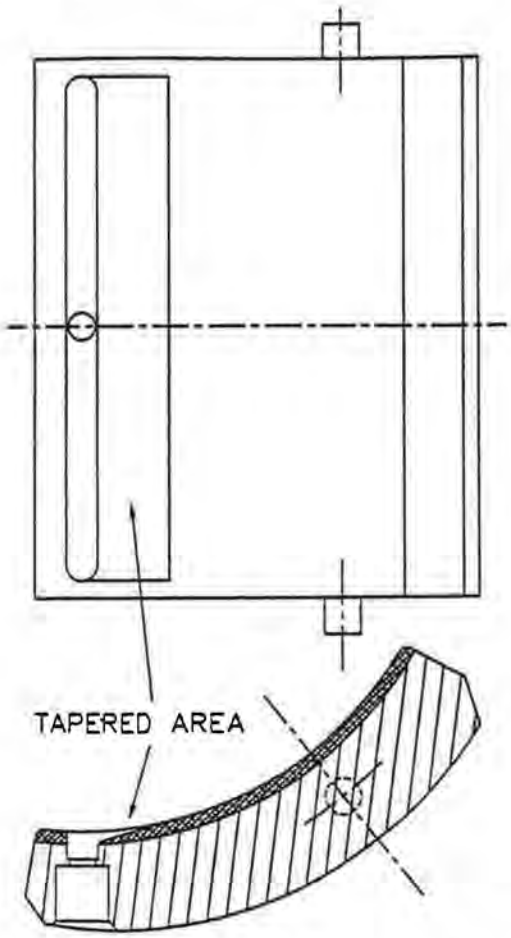

Fig. 7 Sectional View Illustrating Tapered Modification to Leading Edge Groove

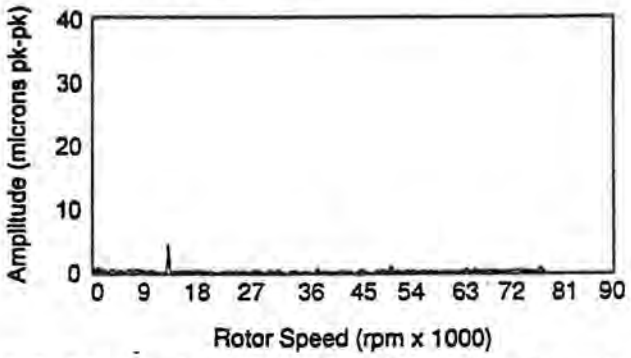

Fig. 8 Frequency Spectrum at 12843 rpm with Tapered Groove – Steam End Left Probe

Unbalance response

During unbalance testing with the tapered groove bearing at the design supply pressure, observed amplitude and amplification factors were reduced at the first peak response speed. Unbalance response data of the original bearing at 15 psig (103.4 kPa) and of the tapered groove design at 7.5 psig (51.7 kPa) are compared in Figure 9. Included in the figure is the predicted response from the original rotordynamics analysis. A summary in Table 1 compares the location, amplification factor, and maximum amplitude of the predicted vs measured peak response speed. This mode was excited by placing two weights of magnitude equal to an unbalance of eight times 4W/N in-phase at the field trim balance planes.

The tapered groove design has a significant improvement on rotor response compared with the original design. This is particularly evident at the first peak response speed, with the maximum amplitude lower by almost a factor of two. The vibration amplitude at the design operating speed is also lower by approximately one half.

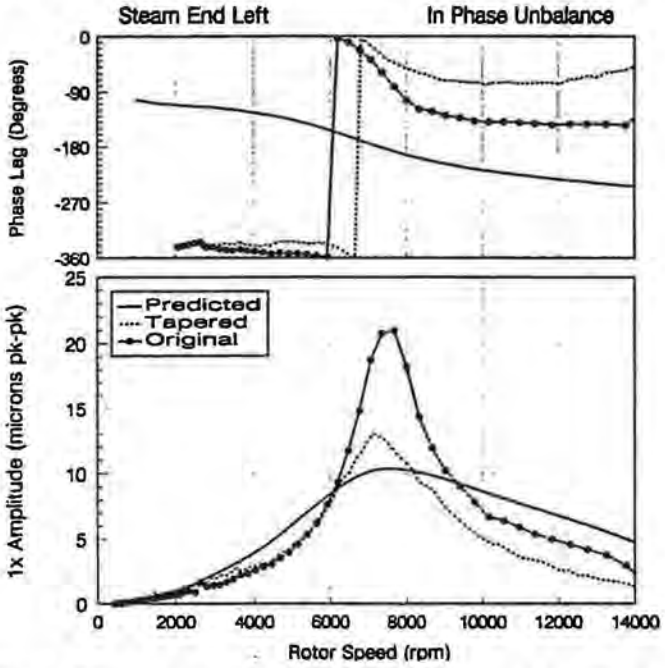

Fig. 9 Comparison of Predicted and Measured Amplitude and Phase Lag at Steam End Left Probe – Original and Tapered Groove Geometries

Accuracy of Theoretical Model

The unbalance response analysis shows that the effective system damping on passing through the first peak response speed is over predicted as measured by amplification factor. The model inaccuracy is also reflected in the stability analysis which indicates a highly stable system. This most likely occurs in the calculation of the stiffness and damping coefficients at these immoderate loads. To some extent, this trend regarding amplification factor has been observed with flooded bearings.

CFD MODELING OF GEOMETRY MODIFICATION

Over the past decade, computational fluid dynamics (CFD) has become the preferred modeling technique for fluid dynamics analysis. CFD provides a method for accurate flow simulation of complex components more quickly and inexpensively than experimental testing. The relative ease of numerical modeling allows for parametric investigation of design modifications, and off-design simulation that may not be experimentally feasible. The CFD results provide detailed properties for the complete flowfield, unlike testing that is limited to discrete instrumentation locations. In modern turbomachinery design, CFD is being actively applied in the modeling of turbine and compressor flowpaths, the simulation of cooling and secondary air flow, and tip leakage reduction, just to name a few. The CFD model results are most meaningful on a relative basis, that is model to model comparisons. The absolute levels from CFD models should be interpreted with caution and ideally calibrated to test data.

CFD Application to Bearing Design

CFD has been applied in hydrodynamic bearing analysis only in very recent years, and in very few applications. The primary reason for the limited use has been the relatively large time involved in the modeling and numerical solution. Bearing specific codes, which have been refined over the last thirty or so years to include effects of turbulence, and thermal and elastic distortion, generally yield accurate results with short setup and run times. Nevertheless, the application of CFD can provide a better understanding of the flow characteristics in bearings. Combined with existing analysis methods, CFD may direct the refinement of design features such as oil supply grooves, taper lands, and pressure dams.

A literature review shows bearing analysis with CFD has concentrated on evaluating thermal effects. These works have generally focused on detailed areas such as oil supply grooves where traditional analysis is dependent on empirical estimates of lumped parameters such as carryover coefficients. The CFD results can provide dimensionless parameter trends applicable to

	Steam End Left			Steam End Right			Exhaust End Left			Exhaust End Right		
	NC_1 (rpm)	AF_1 (dim)	A_{MAX} (μm)	NC_1 (rpm)	AF_1 (dim)	A_{MAX} (μm)	NC_1 (rpm)	AF_1 (dim)	A_{MAX} (μm)	NC_1 (rpm)	AF_1 (dim)	A_{MAX} (μm)
Predicted	7400	1.4	10.7	7600	1.5	10.4	7200	1.4	10.4	7400	1.4	9.9
Original w/103.4 kPa	7678	5.0	21.1	7355	3.5	17.3	7355	4.9	19.8	7355	3.3	16.0
Tapered w/51.7 kPa	7123	3.1	12.9	7623	3.8	14.7	7455	3.4	10.7	7623	3.9	11.9

Table 1 Comparison of Predicted and Measured Peak Response Speed (NC_1), Amplification Factor (AF_1), and Maximum Amplitude (A_{MAX}): Original and Tapered Groove Geometries

generic bearing designs. The usefulness of the CFD work must be weighed against the simplifying assumptions and the significant computational effort.

An early application of CFD in a related area was published by San Andres (1993) to study the thermal performance of cryogenic seals. This work was complimented by Tucker (1995) where CFD was used to validate predictions against published experimental work. Keogh (1996) presented design techniques for thermal prediction in a generic two axial groove journal bearing. A study of pad entrance temperature in a controlled inlet tilting pad thrust bearing was given by Ball (1996). Recently Zhang (1997) presented a thrust bearing design method using CFD.

Hydrodynamic Pressure Distribution Problem

The instability observed on the second application was due to the effect of significantly reduced oil flowrate at the high speed and light load conditions. A CFD model was proposed to investigate the flow mechanisms of the instability. The difficulties of modeling a tilting pad journal bearing are many; the highly complex, three dimensional flowfield and unknown boundary conditions to name a few.

A tilting pad journal bearing consists of a housing that supports several pads that can individually tilt with respect to one another. The pads are designed with a bore that is oversized compared to the assembled bearing bore to facilitate the development of an oil film wedge. The pads in the lower half of the bearing tilt and generate a hydrodynamic force that supports the weight of the rotor and the effect of any downward load from the pads in the upper half. The end result is a system that is in steady state equilibrium under the operating speed and load conditions imposed.

Description of the Model

The objective of the CFD model was to understand the pad geometry effects on the flowfield through the supply tube and into the clearance between the journal and pad. The ideal model would be a 3-D simulation of the full bearing. Limited resources and boundary conditions provided the dose of realism to direct the model to a 2-D slice of a single pad. The CFD analysis used a baseline model defined by the original pad geometry. This model formed the comparison basis for the second model with the modified pad geometry. A 2-D slice, 0.005 inch (0.127 mm) wide, through the bearing axial center defined the geometry. This slice incorporates the features of interest; the oil supply hole and axial feed groove. Even with this small thickness, the models were approximately 8500 elements to provide adequate resolution through the small journal-to-pad clearance.

The CFD model was set up to evaluate one of the loaded pads. The model was constructed by setting the oil film thickness at the pivot to 5 mil (0.127 mm), and then rotating the pad geometry 0.1 degree in the direction of rotation to represent the oil film wedge. The pivot film thickness and angle of tilt were determined by a conventional tilting pad journal bearing analysis program. A sectional view of the grid mesh used in the analysis of the original groove geometry is illustrated in Figure 10, the tapered modification in Figure 11.

A commercial CFD software package (TASCflow, 1996) was used to develop the models and provide the numerical solution. The code is a finite volume method which solves the 3-D

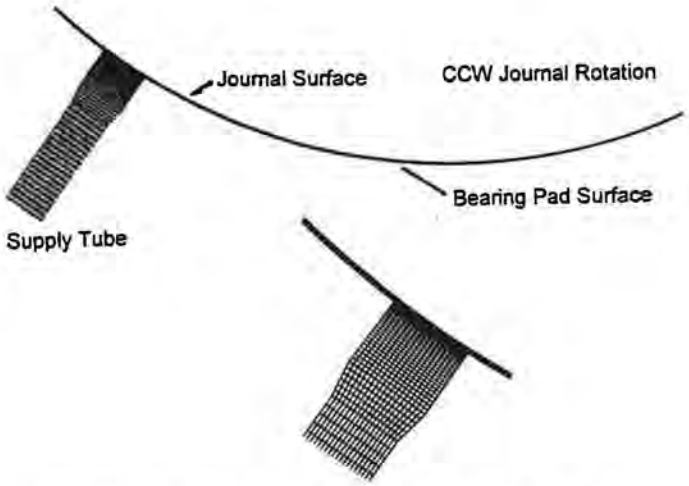

Fig. 10 Original Groove Geometry Grid Mesh

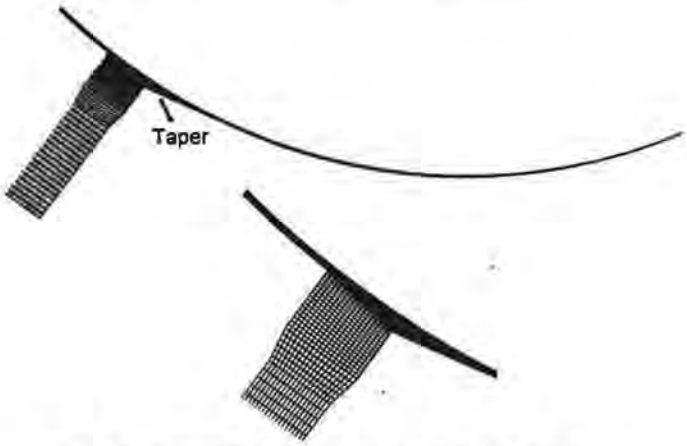

Fig. 11 Tapered Groove Geometry Grid Mesh

Reynolds-averaged Navier-Stokes equations for fluid flow within complex geometries.

Boundary Conditions and Solution Technique

A simplifying assumption was axial flow is insignificant compared to the throughflow. This is appropriate given the model location and the goal to evaluate pad geometry changes. The model accounts for the journal rotation, turbulence (k-ε model), and viscous shearing. At each node, velocity, k-ε turbulence, pressure, and temperature were calculated. The fluid properties were based on published data for a typical light lubricant oil.

The supply tube opening was defined as the inlet boundary. The inlet boundary condition was set with pressure at 7.5 psig (51.7 kPa) to represent the test. This inlet pressure was adjusted in the second model to match the baseline flow rate. The pad leading and trailing edges were defined to allow inflow or outflow. The boundary conditions were set with pressure to ambient to match test conditions.

The desired solution at the high rotational speed was obtained by ramping up the speed. Flow solutions were obtained at speed increments to provide starting conditions for the new

speed. This technique of simulating a startup proved successful for stable, convergent solutions.

Evaluation of Original Groove Geometry

Figure 12 is a flow visualization of the velocity field at a shaft speed of 12000 rpm. A flow vortex or recirculation is apparent in the region of the feed groove; the rotation is in the same direction with the journal. The vortex is generated by the shearing of the oil as it attempts to penetrate the journal oil film. The oil is peeled off the journal film by the aft corner of the feed groove. This is particularly evident in Figure 13 which shows streaklines initiated at the inlet boundary. The path of one of the streaklines bounds the recirculation zone and does not penetrate the oil film. Additional insight is provided by the temperature contours in Figure 14 which show a corresponding hot spot in the feed groove.

A particular interest is the pressure profile of the oil film, shown in Figure 15. The pressure in the small pad area upstream of the feed groove is less than the supply. The lower pressure is sensible with the feed groove recirculation. The pressure increases to a constant value equal to the supply across the feed groove. Moving downstream, the pressure increases to a maximum near the pivot and then rapidly drops to ambient.

The original hypothesis was that the instability was caused by the pad attitude angle approaching zero. This was investigated with the original groove model by setting the pad attitude angle to zero. The pivot film thickness was left at 5 mil (0.127 mm). The zero pad angle provides a convergent region upstream of the pivot (with respect to the direction of journal rotation) and divergent downstream of the pivot. Although the analysis on this configuration converged to a steady state solution at the lower rotational speeds, it did not at the higher speeds. The coincidence of the time periodic nature of the unconverged solution and the observed vibration instability, supports the hypothesis that the vibration instability was due to a highly centered bearing.

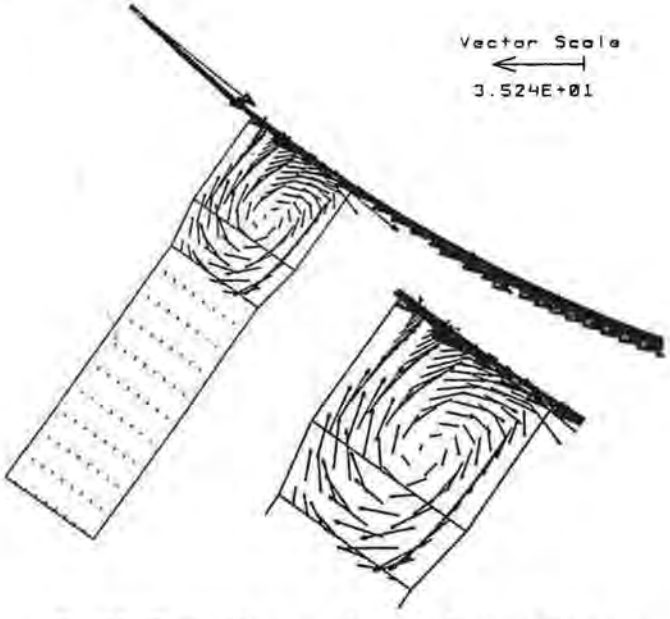

Fig. 12 Speed Vectors – Original Groove Geometry

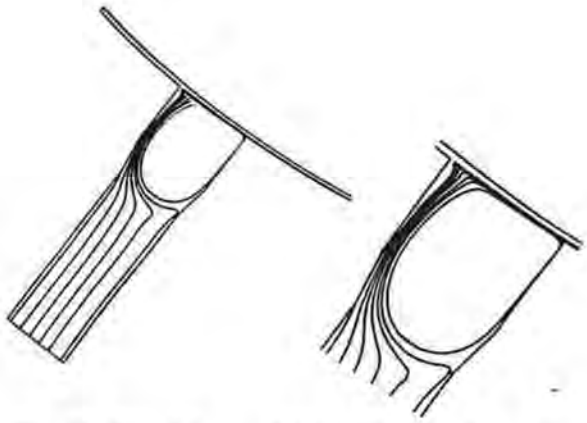

Fig. 13 Streaklines – Original Groove Geometry

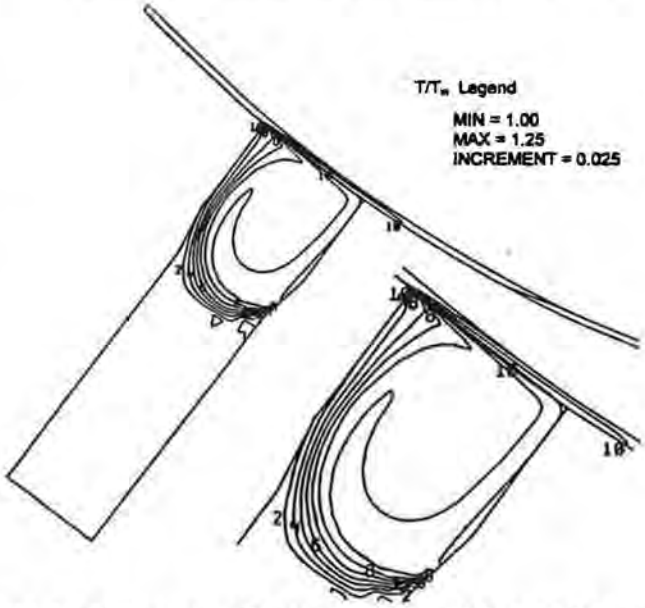

Fig. 14 Temperature Contours – Original Groove Geometry

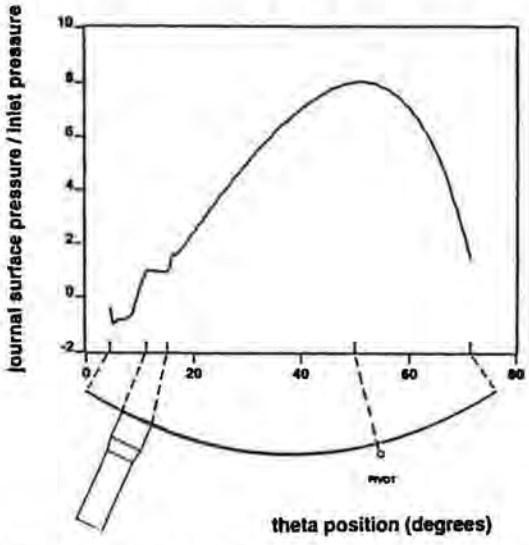

Fig. 15 Pressure Profile – Original Groove Geometry

Evaluation of Tapered Groove Geometry

The results, using identical boundary conditions and pad attitude angle, for the tapered groove pad geometry are given in Figures 16 to 19. The velocity field plot on Figure 16 shows a recirculating zone in the feed groove as was shown with the original geometry. The recirculation is now rotating in the opposite direction to the journal. The recirculation strength and penetration is reduced compared to the original geometry. The peeling of the journal film by the aft edge of the feed groove is greatly reduced with the taper. There likely is an optimum taper geometry that will minimize or eliminate the journal film peeling and recirculation; this aspect was not investigated in this study.

A revealing effect of the tapered geometry is shown by the journal pressure profile comparison in Figure 19. The small upstream pad area shows a pressure increase over the baseline model; this corresponds with the change of rotation in the recirculation zone. The pressure step at the feed groove exit in the original geometry is eliminated with the taper modification. Downstream of the feed groove the maximum hydrodynamic pressure has increased 40 percent compared to the original geometry; the location has moved downstream of the pivot. A principle conclusion is that the taper does promote hydrodynamic pressure generation, and does not simply increase the hydrostatic force in the area adjacent to the feed groove.

In reality the bearing pads will tilt to a position of equilibrium. The pad attitude angles with the tapered geometry will, therefore, adjust to seek a new equilibrium position. The results of the CFD comparison at the same attitude angle are qualitative only, and do not necessarily reflect the actual dynamic behavior of the modified bearing.

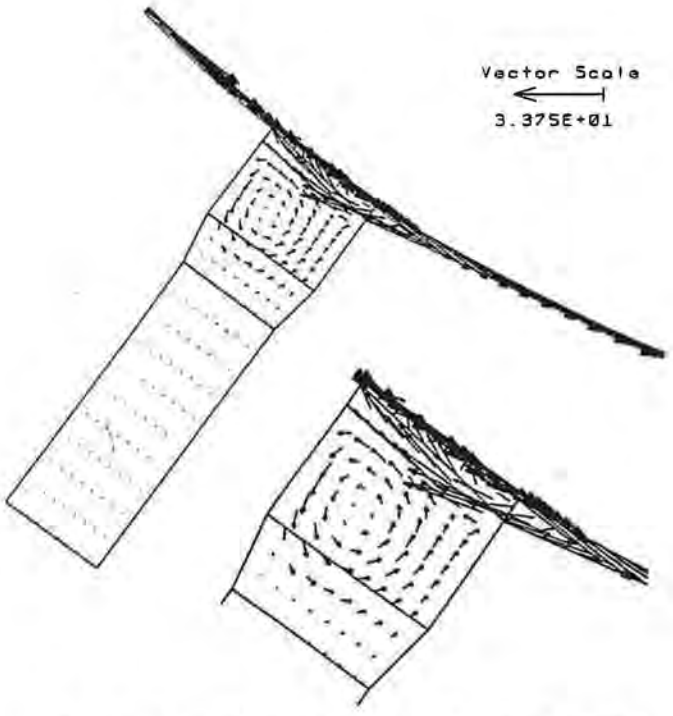

Fig. 16 Speed Vectors – Tapered Groove Geometry

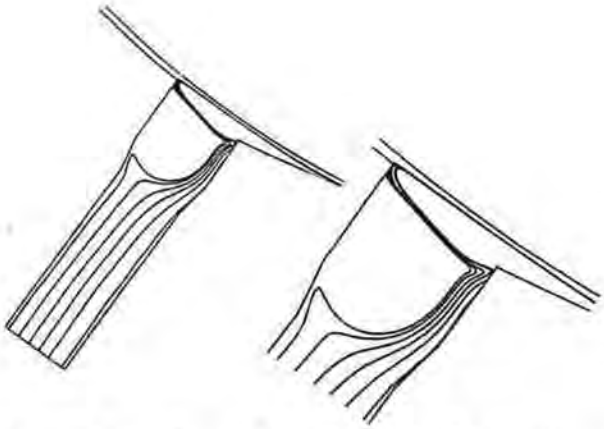

Fig. 17 Streaklines – Tapered Groove Geometry

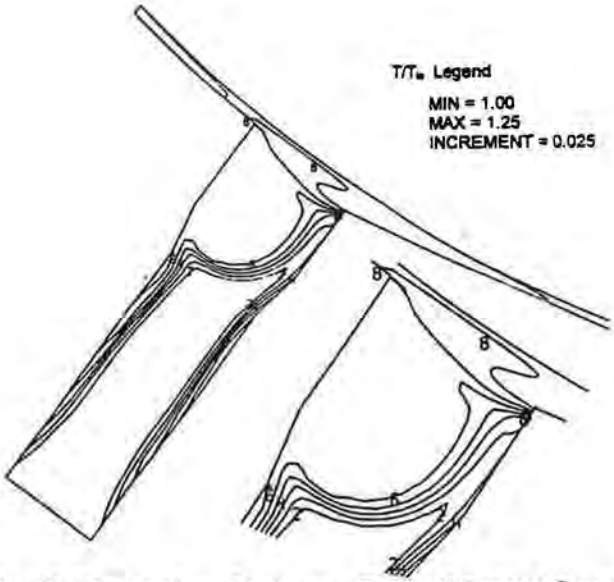

Fig. 18 Temperature Contours – Tapered Groove Geometry

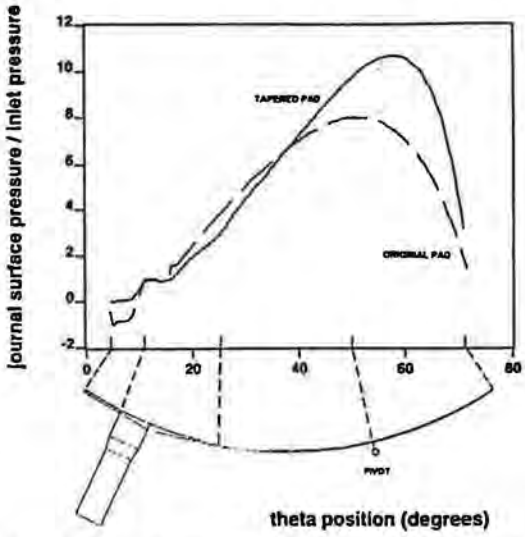

Fig. 19 Pressure Profile – Tapered Groove Geometry

CONCLUSIONS

- Current rotor-bearing analysis techniques are not infallible. The case history presented complied with all generally accepted rotordynamics criteria. The test, however, exhibited an instability and higher than predicted vibration on passing through the first lateral natural frequency.
- The dynamic performance of a rotor supported on leading edge groove bearings was improved by adding a taper to the exit side of the feed groove of each pad. The observed benefits were lower vibration amplitudes and improved rotor-bearing stability.
- CFD can provide additional insight into the fluid dynamic characteristics of a tilting pad journal bearing. A disadvantage compared to conventional bearing codes is the additional time it takes to setup and run an analysis.
- The CFD results show the addition of a taper to the exit side of the leading edge groove greatly changed the characteristic of the hydrodynamic oil film. It is postulated that this is the mechanism that produced the observed improvement in the response of the rotor-bearing system.
- A particularly useful result from CFD is the detailed visualization of the thermal behavior not available from established bearing analysis codes. In this study, a recirculation zone was observed in the feed groove that influences the pad entrance temperature.
- CFD results can provide important information for bearing design optimization. This was shown by the comparison of the two models in this study.
- The taper modification was proven on a very lightly loaded tilting pad journal bearing with a projected load of less than 25 psi (172 kPa). The effect at higher bearing load was not investigated.

ACKNOWLEDGEMENTS

The authors would like to thank colleagues at Dresser-Rand Steam Turbine Division and Kingsbury, Inc. for their comments throughout this project. The CFD model guidance provided by the application specialists at AEA-ASC is also gratefully acknowledged.

REFERENCES

Adams, M. L. and Payandeh, S., 1983, "Self-Excited Vibration of Statically Unloaded Pads in Tilting-Pad Journal Bearings," ASME Journal of Lubrication Technology, Vol. 105, pp. 377-384.

American Petroleum Institute Standard 612, 1995, "Special Purpose Steam Turbines for Refinery Services," American Petroleum Institute, Washington D. C., Fourth Edition.

Ball, J. H., 1996, "Design Considerations for Thrust Bearing Applications," Proceedings of the Twenty Fifth Turbomachinery Symposium, The Turbomachinery Laboratory, Texas A&M University, College Station, Texas.

Dmochowski, W., Brockwell, K., DeCamillo, S., and Mikula, A., 1993, "A Study of the Thermal Characteristics of the Leading Edge Groove and Conventional Tilting Pad Journal Bearings," ASME Journal of Tribology, Vol. 115, pp. 219-226.

Edney, S. L., 1995, "Pad Temperature in High Speed, Lightly Loaded Tilting Pad Journal Bearings," Proceedings of the Twenty Fourth Turbomachinery Symposium, The Turbomachinery Laboratory, Texas A&M University, College Station, Texas.

Edney, S. L., Waite, J. K., and DeCamillo, S., 1996, "Profiled Leading Edge Groove Tilting Pad Journal Bearing for Light Load Operation," Proceedings of the Twenty Fifth Turbomachinery Symposium, The Turbomachinery Laboratory, Texas A&M University, College Station, Texas.

Harangozo, A. V., Stolarski, T. A., and Gozdawa, R. J., 1991, "The Effect of Different Lubrication Methods on the Performance of a Tilting Pad Journal Bearing," STLE Tribology Transactions, Vol. 34, pp. 529-536.

Keogh, P. S., Gomiciaga, R., and Khonsari, M. M., 1996, "CFD Based Design Techniques for Thermal Prediction in a Generic Two Axial Groove Hydrodynamic Journal Bearing," ASME/STLE Tibology Conference, San Francisco, California.

Mikula, A. and Gregory, R., 1981, "A Comparison of Thrust Bearing Lubricant Supply Methods," ASME Journal of Lubrication Technology, Vol. 105, pp. 39-47.

Nicholas, J. C., 1994, "Tilting Pad Bearing Design," Proceedings of the Twenty Third Turbomachinery Symposium, The Turbomachinery Laboratory, Texas A&M University, College Station, Texas.

San Andres, L., Yang, Z., and Childs, D. W., 1993, "Thermal Effects in Cryogenic Liquid Annular Seals - Part II: Numerical Solution and Results," ASME Journal of Tribology, Vol. 116, pp. 277-284.

Tanaka, M., 1991, "Thermohydrodynamic Performance of a Tilting Pad Journal Bearing with Spot Lubrication," ASME Journal of Tribology, Vol. 113, pp. 615-619.

TASCflow, 1996, AEA Technolgy, Advanced Scientific Computing, Waterloo, Ontario, Canada.

Tucker, P. G. and Keogh, P. S., 1995, "A Generalized CFD Approach for Journal Bearing Performance Prediction," Proceedings of the Institution of Mechanical Engineers, Journal of Tribology, Vol. 209, Part J, pp. 99-108.

Tucker, P. G. and Keogh, P. S., 1995, "On the Dynamic Thermal State in a Hydrodynamic Bearing with a Whirling Journal Using CFD Techniques," ASME/STLE Tribology Conference, Orlando, Florida.

Zhang, J.X. and Rodkiewicz, C.M., 1997, "On the Design of Thrust Bearings Using a CFD Technique," Vol. 40, pp. 403-412.